



Synthesis of a Spatially Band-Limited Plane Wave in the Time-Domain Using Wave Field Synthesis

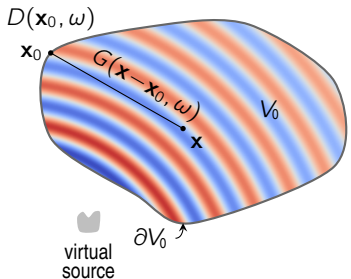
Nara Hahn, Fiete Winter, and Sascha Spors

Institute of Communications Engineering
University of Rostock, Germany



30. August 2017, Kos, Greece

Wave Field Synthesis (WFS)



$S(\mathbf{x}, \omega)$	desired sound field
$D(\mathbf{x}_0, \omega)$	driving function
$G(\mathbf{x} - \mathbf{x}_0, \omega)$	spatial transfer function
V_0	listening area/volume

- an analytic method for sound field synthesis [Berkhout et al., 1993, Spors et al., 2008]

$$S(\mathbf{x}, \omega) = \oint_{\partial V_0} D(\mathbf{x}_0, \omega) G(\mathbf{x} - \mathbf{x}_0, \omega) dA, \quad \mathbf{x} \in V_0$$

- based on the Rayleigh integral equation

$$S(\mathbf{x}, \omega) = \iint_{-\infty}^{\infty} \underbrace{-2 \frac{\partial}{\partial n_0} S(\mathbf{x}_0, \omega) G(\mathbf{x} - \mathbf{x}_0, \omega)}_{D_{WFS}(\mathbf{x}_0, \omega)} d\mathbf{x}_0 dz_0, \quad y > y_0$$

- analytic solution for linear/planar arrays
- approximated solution for arbitrary convex-shaped arrays (high-frequency approximation)

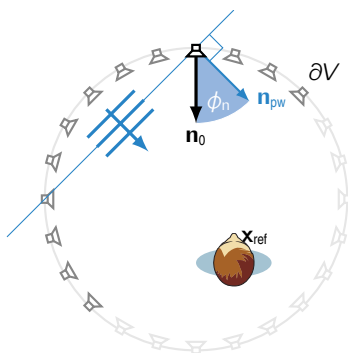
Synthesis of a Virtual Plane Wave

2.5D Driving Function

[Spors et al., 2008, Schultz, 2016]

$$\text{frequency domain} \quad D(\mathbf{x}, \omega) = \sqrt{i \frac{\omega}{c}} a(\mathbf{x}_0) \sqrt{8\pi} \sqrt{\|\mathbf{x}_0 - \mathbf{x}_{\text{ref}}\|} \langle \mathbf{n}_{\text{pw}}, \mathbf{n}_0(\mathbf{x}_0) \rangle e^{-i \frac{\omega}{c} \langle \mathbf{n}_{\text{pw}}, \mathbf{x}_0 \rangle}$$

$$\text{time domain} \quad d(\mathbf{x}, t) = \underbrace{h_{\text{pre}}(t)}_{\text{pre-equalization filter}} *_t \underbrace{a(\mathbf{x}_0)}_{\text{secondary source selection}} \underbrace{\sqrt{8\pi} \sqrt{\|\mathbf{x}_0 - \mathbf{x}_{\text{ref}}\|} \langle \mathbf{n}_{\text{pw}}, \mathbf{n}_0(\mathbf{x}_0) \rangle}_{\text{amplitude correction @ } \mathbf{x}_{\text{ref}}} \underbrace{\cos \phi_n}_{\text{cos } \phi_n} \underbrace{\delta\left(t - \frac{\langle \mathbf{n}_{\text{pw}}, \mathbf{x}_0 \rangle}{c}\right)}_{\text{delay}}$$



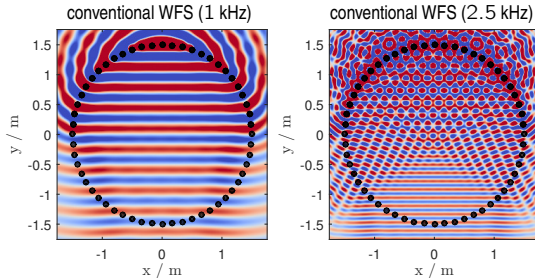
\mathbf{n}_0 inward pointing normal vector

\mathbf{n}_{pw} plane wave direction

$\phi_n = \arccos(\langle \mathbf{n}_{\text{pw}}, \mathbf{n}_0 \rangle)$

$a(\mathbf{x}_0)$ 1 or 0

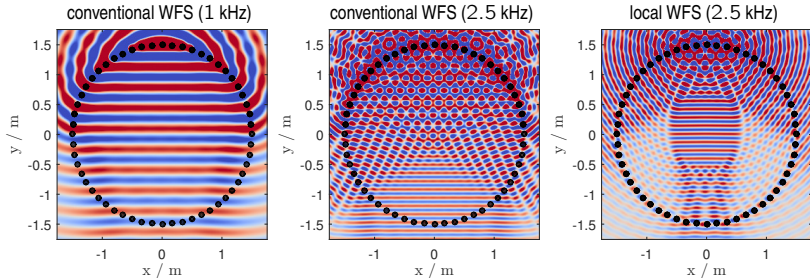
Spatial Aliasing and Local WFS



[circular array $R = 1.5$, 56 loudspeakers, $\phi_{\text{pw}} = -90^\circ$]

- using a finite number of loudspeakers results in spatial aliasing artifacts ($f > f_{\text{al}}$)
- local WFS achieves increased accuracy within a local area
 1. virtual loudspeaker array [Spors and Ahrens, 2010]
 2. virtual equivalent scattering and time reversal [Spors et al., 2011]
 3. spatial band-limitation [Hahn et al., 2016]

Spatial Aliasing and Local WFS

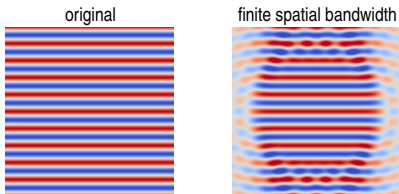


[circular array $R = 1.5$, 56 loudspeakers, $\phi_{pw} = -90^\circ$]

- using a finite number of loudspeakers results in spatial aliasing artifacts ($f > f_{al}$)
- local WFS achieves increased accuracy within a local area
 1. virtual loudspeaker array [Spors and Ahrens, 2010]
 2. virtual equivalent scattering and time reversal [Spors et al., 2011]
 3. spatial band-limitation [Hahn et al., 2016]

Local WFS by Spatial Band-Limitation in the Circular Harmonics Domain

[Hahn et al., 2016]



- circular harmonics expansion of a plane wave with respect to \mathbf{x}_c

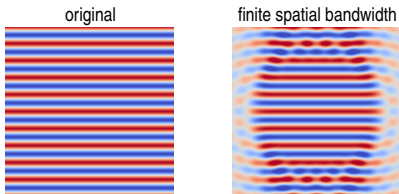
$$e^{-i\frac{\omega}{c}\langle \mathbf{n}_{pw}, \mathbf{x} \rangle} = e^{-i\frac{\omega}{c}\langle \mathbf{n}_{pw}, \mathbf{x}_c \rangle} \sum_{m=-\infty}^{\infty} \underbrace{i^{-m} e^{-im\phi_{pw}}}_{\text{expansion coefficient}} \underbrace{J_m\left(\frac{\omega}{c}r'\right)}_{\text{Bessel function}} \underbrace{e^{im\phi'}}_{\text{circular harmonics}}, \quad \text{where } \mathbf{x} - \mathbf{x}_c = (r', \phi', z')$$

spatial band-limitation: M \Rightarrow describes the sound field within a circular region $r_M \approx \frac{cM}{2\pi f}$ [Kennedy et al., 2007]

- WFS driving function based on spatially band-limited circular harmonics expansion
- driving function available only in the frequency domain so far 😞

Local WFS by Spatial Band-Limitation in the Circular Harmonics Domain

[Hahn et al., 2016]



- circular harmonics expansion of a plane wave with respect to \mathbf{x}_c

$$e^{-i\frac{\omega}{c}\langle \mathbf{n}_{pw}, \mathbf{x} \rangle} \approx e^{-i\frac{\omega}{c}\langle \mathbf{n}_{pw}, \mathbf{x}_c \rangle} \sum_{m=-M}^M \underbrace{i^{-m} e^{-im\phi_{pw}}}_{\text{expansion coefficient}} \underbrace{J_m\left(\frac{\omega}{c}r'\right)}_{\text{Bessel function}} \underbrace{e^{im\phi'}}_{\text{circular harmonics}}, \quad \text{where } \mathbf{x} - \mathbf{x}_c = (r', \phi', z')$$

spatial band-limitation: $M \Rightarrow$ describes the sound field within a circular region $r_M \approx \frac{cM}{2\pi f}$ [Kennedy et al., 2007]

- WFS driving function based on spatially band-limited circular harmonics expansion
- driving function available only in the frequency domain so far 😞

Time-Domain Representation I

Circular Harmonics Expansion ($x_c = 0$)

$$S(x, \omega) = \sum_{m=-M}^M i^{-m} e^{-im\phi_{pw}} J_m(\frac{\omega}{c}r) e^{im\phi}$$

Plane Wave Decomposition

$$S(x, \omega) = \frac{1}{2\pi} \int_0^{2\pi} \mathcal{D}_M(\alpha - \phi_{pw}) e^{-i\frac{\omega}{c}r \cos(\phi - \alpha)} d\alpha$$

$$\text{where } \mathcal{D}_M(\alpha - \phi_{pw}) \equiv \sin\left(\frac{2M+1}{2}(\alpha - \phi_{pw})\right) / \sin\left(\frac{1}{2}(\alpha - \phi_{pw})\right)$$

$\downarrow \mathcal{F}_t^{-1}$

$$s(x, t) = \frac{1}{2\pi} \int_0^{2\pi} \mathcal{D}_M(\alpha - \phi_{pw}) \delta\left(t - \frac{r}{c} \cos(\phi - \alpha)\right) d\alpha$$

\downarrow WFS Driving Function

$$d_{PWD}(x_0, t) = \sqrt{\frac{2r}{\pi}} \int_0^{2\pi} a(x_0, \alpha) \langle n_\alpha, n_0 \rangle \\ \times \mathcal{D}_M(\alpha - \phi_{pw}) \delta\left(t - \frac{r}{c} \cos(\phi - \alpha)\right) d\alpha$$

Time-Domain Representation II

$$s(x, t) = \frac{1}{2\pi} \int_0^{2\pi} \mathcal{D}_M(\alpha - \phi_{pw}) \delta(t - \frac{r}{c} \cos(\phi - \alpha)) d\alpha$$

↓ sifting property of $\delta(\cdot)$

$$s(x, t) = \frac{1}{2\pi} \frac{\Pi(\frac{ct}{2r})}{|\sin \beta(t)|} [\mathcal{D}_M(\phi - \phi_{pw} - \pi + \beta(t)) \delta(t - \frac{r}{c} \cos(\beta(t) + \pi)) \\ + \mathcal{D}_M(\phi - \phi_{pw} - \pi - \beta(t)) \delta(t - \frac{r}{c} \cos(-\beta(t) + \pi))]$$

where $\beta(t) = \arccos\left(-\frac{ct}{r}\right)$ and $\Pi(\cdot)$: rectangular function

↑ \mathcal{F}^{-1}

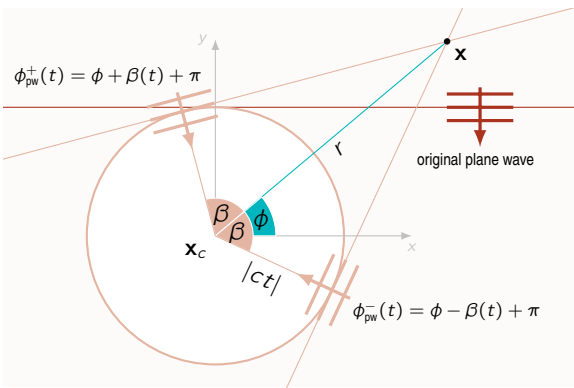
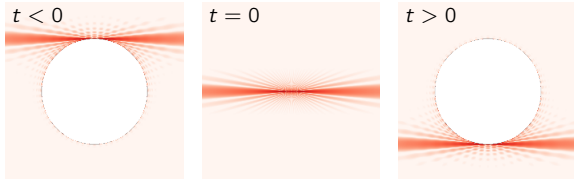
Circular Harmonics Expansion

- two plane waves at each time instance for $-\frac{r}{c} < t < \frac{r}{c}$

$$\phi_{pw}^+(t) = \phi + \beta(t) + \pi$$

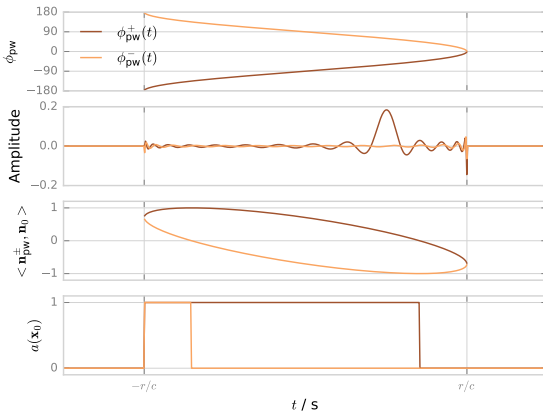
$$\phi_{pw}^-(t) = \phi - \beta(t) + \pi$$

Spatially Band-Limited Plane Wave



WFS Driving Function

$$d(x_0, t) = \sqrt{\frac{2r}{\pi}} \frac{\Pi(\frac{ct}{2r})}{|\sin \beta(t)|} \times \left[a(x_0, \phi_{pw}^+(t)) \langle n_{pw}^+(t), n_0 \rangle \mathcal{D}_M(\phi_{pw}^+(t)) + a(x_0, \phi_{pw}^-(t)) \langle n_{pw}^-(t), n_0 \rangle \mathcal{D}_M(\phi_{pw}^-(t)) \right]$$



$$[x_c = (0, 0, 0), x_0 = (1.5, 0, 0), \phi_{pw} = -\frac{\pi}{3}, \phi_n = -\frac{3\pi}{4}]$$

Practical Implementation

PWD

$$d_{\text{PWD}}(x_0, t) = \sqrt{\frac{2r}{\pi}} \int_0^{2\pi} a(x_0, \alpha) \langle n_\alpha, n_0 \rangle \\ \times \mathcal{D}_M(\alpha - \phi_{\text{pw}}) \delta(t - \frac{r}{c} \cos(\phi - \alpha)) d\alpha$$

CHT

$$d_{\text{CHT}}(x_0, t) = \sqrt{\frac{2r}{\pi}} \frac{\Pi(\frac{ct}{2r})}{|\sin \beta(t)|} \times \left[a(x_0, \phi_{\text{pw}}^+(t)) \langle n_{\text{pw}}^+(t), n_0 \rangle \mathcal{D}_M(\phi_{\text{pw}}^+(t)) \right. \\ \left. + a(x_0, \phi_{\text{pw}}^-(t)) \langle n_{\text{pw}}^-(t), n_0 \rangle \mathcal{D}_M(\phi_{\text{pw}}^-(t)) \right]$$

- temporal sampling: integer or fractional delay
- spatial sampling: synthesize only a finite number of plane waves e.g. equi-angular sampling
- temporal sampling implicitly discretizes the plane wave angles constitutes a nonuniform sampling of ϕ_{pw}^\pm
- anti-aliasing filtering and dynamic range control using $\arctan(\cdot)$

$$\mathcal{L}(u) = \frac{2A_{\text{thr}}}{\pi} \arctan \left(\frac{\pi u}{2A_{\text{thr}}} \right)$$

Practical Implementation

PWD

$$d_{\text{PWD}}(x_0, t) = \sqrt{\frac{2r}{\pi}} \int_0^{2\pi} a(x_0, \alpha) \langle n_\alpha, n_0 \rangle \\ \times \mathcal{D}_M(\alpha - \phi_{\text{pw}}) \delta(t - \frac{r}{c} \cos(\phi - \alpha)) d\alpha$$

CHT

$$d_{\text{CHT}}(x_0, t) = \sqrt{\frac{2r}{\pi}} \frac{\Pi(\frac{ct}{2r})}{|\sin \beta(t)|} \times \left[a(x_0, \phi_{\text{pw}}^+(t)) \langle n_{\text{pw}}^+(t), n_0 \rangle \mathcal{D}_M(\phi_{\text{pw}}^+(t)) \right. \\ \left. + a(x_0, \phi_{\text{pw}}^-(t)) \langle n_{\text{pw}}^-(t), n_0 \rangle \mathcal{D}_M(\phi_{\text{pw}}^-(t)) \right]$$

- temporal sampling: integer or fractional delay
- spatial sampling: synthesize only a finite number of plane waves e.g. equi-angular sampling
- temporal sampling implicitly discretizes the plane wave angles constitutes a nonuniform sampling of ϕ_{pw}^\pm
- anti-aliasing filtering and dynamic range control using $\arctan(\cdot)$

$$\mathcal{L}(u) = \frac{2A_{\text{thr}}}{\pi} \arctan \left(\frac{\pi u}{2A_{\text{thr}}} \right)$$

2.5D WFS Simulation

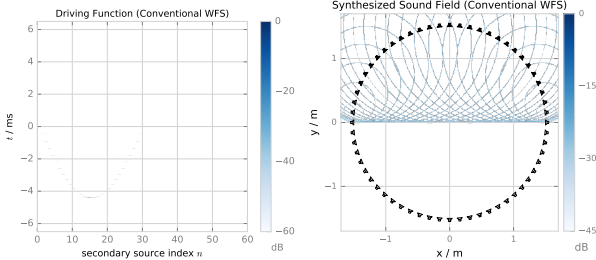
Configuration

- circular array $R = 1.5 \text{ m}$, $N = 60$ loudspeakers
- virtual plane wave $\phi_{\text{pw}} = -90^\circ$ (downwards)
- spatial bandwidth $M = 29$
- sampling frequency $f_s = 44.1 \text{ kHz}$

Driving Functions

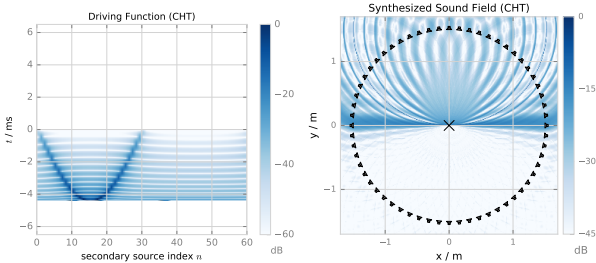
- conventional WFS
 - circular harmonics expansion (CHT)
 - plane wave decomposition using *integer delay* (PWD-i)
 - plane wave decomposition using *fractional delay* (PWD-f) 20th-order Lagrange polynomial
- † number of plane waves ($N_{\text{pw}} = 385$) matched for CHT, PWD-i, and PWD-f

Driving Function and Synthesized Sound Field



- Conventional WFS
 - driving function given as delay and weight
 - straight wavefront followed by spatial aliasing components
- Spatially band-limited WFS
 - peaks of the driving function always on the v-shaped contour
 - detailed structure depends on the expansion center of the circular harmonics expansion
 - improved accuracy around x_c

Driving Function and Synthesized Sound Field



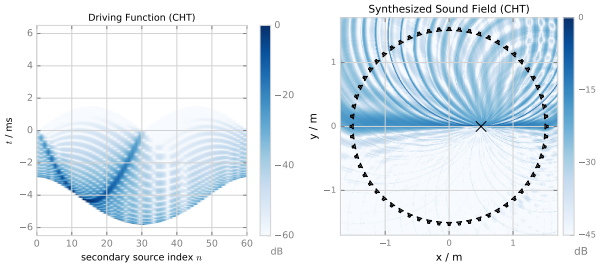
- Conventional WFS

- driving function given as delay and weight
- straight wavefront followed by spatial aliasing components

- Spatially band-limited WFS

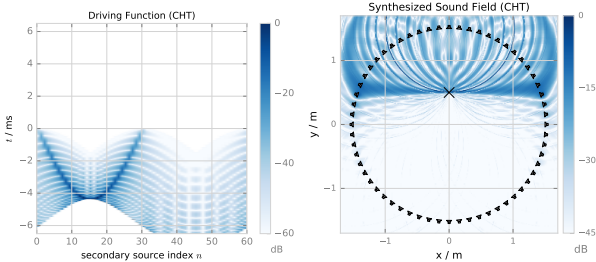
- peaks of the driving function always on the v-shaped contour
- detailed structure depends on the expansion center of the circular harmonics expansion
- improved accuracy around \times_c

Driving Function and Synthesized Sound Field



- Conventional WFS
 - driving function given as delay and weight
 - straight wavefront followed by spatial aliasing components
- Spatially band-limited WFS
 - peaks of the driving function always on the v-shaped contour
 - detailed structure depends on the expansion center of the circular harmonics expansion
 - improved accuracy around x_c

Driving Function and Synthesized Sound Field



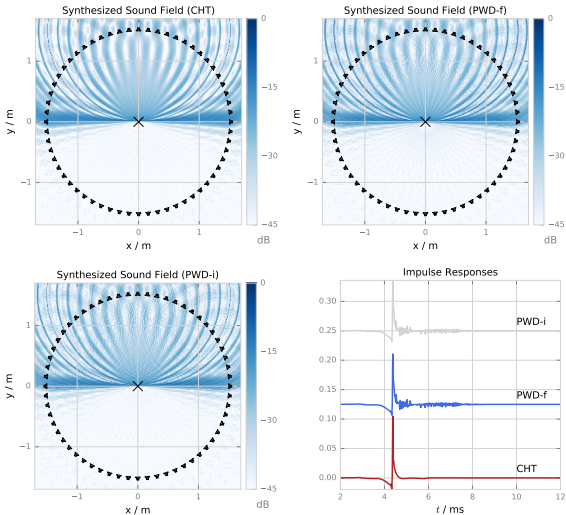
- Conventional WFS

- driving function given as delay and weight
- straight wavefront followed by spatial aliasing components

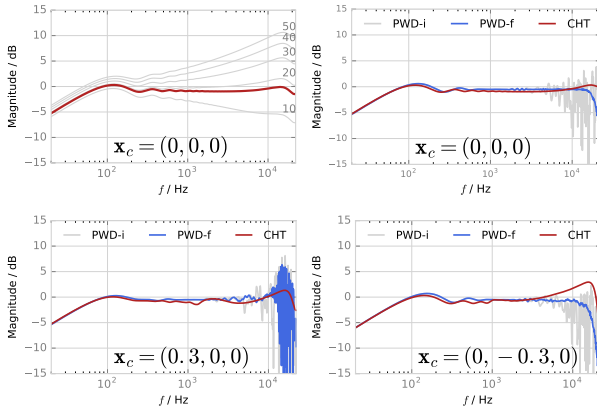
- Spatially band-limited WFS

- peaks of the driving function always on the v-shaped contour
- detailed structure depends on the expansion center of the circular harmonics expansion
- improved accuracy around x_c

Temporal Properties

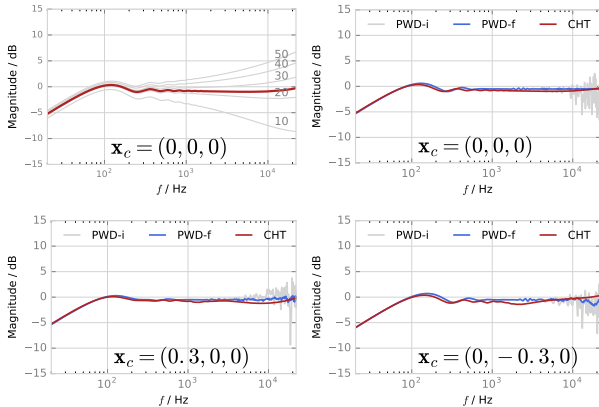


Spectral Properties



- CHT: optimal $A_{\text{thr}} = 17$ found empirically
- CHT: high-frequency deviations (< 3 dB) due to temporal aliasing
- PWD-i & PWD-f: fluctuations at high frequencies
- typical low-frequency deviation in WFS due to high-frequency approximation

Improvement by Oversampling $\uparrow 2$



- CHT: $A_{\text{thr}} = 24$
- $f_s = 88.2 \text{ kHz}$, $N_{\text{pw}} = 771$
- CHT: outperforms PWD-i and comparable to PWD-f
- PWD-f: computational complexity increases significantly

Conclusion

Summary

- two time-domain representations introduced (CHT & PWD) for a spatially band-limited plane
- corresponding WFS driving functions derived
- improved accuracy achieved within a freely movable local listening area
- CHT, PWD-i, and PWD-f compared in terms of temporal/spectral/spatial properties

Future Work

- CHT: improved anti-aliasing filtering and dynamic range control
- physical/perceptual comparison with other local WFS methods

What about POINT SOURCES?

⇒ Fiete Winter et al., "*Time-Domain Realisation of Model-Based Rendering for 2.5D Local Wave Field Synthesis Using Spatial Bandwidth-Limitation*" [AASP-L3, 11:00, Aegle B]

References I

-  Abramowitz, M. and Stegun, I. A. (1964).
Handbook of Mathematical Functions: with Formulas, Graphs, and Mathematical Tables.
Number 55. Courier Corporation.
-  Berkhout, A. J., de Vries, D., and Vogel, P. (1993).
Acoustic Control by Wave Field Synthesis.
J. Acoust. Soc. Am. (JASA), 93(5):2764–2778.
-  Hahn, N., Winter, F., and Spors, S. (2016).
Local Wave Field Synthesis by Spatial Band-limitation in the Circular/Spherical Harmonics Domain.
In *Proc. 140th Audio Eng. Soc. (AES) Conv.*, Paris, France.
-  Kennedy, R. A., Sadeghi, P., Abhayapala, T. D., and Jones, H. M. (2007).
Intrinsic Limits of Dimensionality and Richness in Random Multipath Fields.
IEEE Trans. Signal Process., 55(6):2542–2556.
-  Schultz, F. (2016).
Sound Field Synthesis for Line Source Array Applications in Large-Scale Sound Reinforcement.
PhD thesis, University of Rostock.
-  Spors, S. and Ahrens, J. (2010).
Analysis and Improvement of Pre-equalization in 2.5-dimensional Wave Field Synthesis.
In *Proc. 128th Audio Eng. Soc. (AES) Conv.*, London, UK.

References II



Spors, S., Helwani, K., and Ahrens, J. (2011).

Local Sound Field Synthesis by Virtual Acoustic Scattering and Time-reversal.

In *Proc. 131th Audio Eng. Soc. (AES) Conv.*, New York, USA.



Spors, S., Rabenstein, R., and Ahrens, J. (2008).

The Theory of Wave Field Synthesis Revisited.

In *Proc. 124th Audio Eng. Soc. (AES) Conv.*

Circular Harmonics Expansion of a Plane Wave

- plane wave with angle ϕ_{pw} and wave vector $\mathbf{k}_{pw} = [\frac{\omega}{c} \cos \phi_{pw}, \frac{\omega}{c} \sin \phi_{pw}, 0]^T$ (parallel to the xy -plane)
- \mathbf{x}_c : expansion center
- approximated with a final number of terms M

$$\begin{aligned} e^{-i\langle \mathbf{k}_{pw}, \mathbf{x} \rangle} &= \sum_{m=-\infty}^{\infty} i^{-m} e^{im\phi_{pw}} \underbrace{J_m\left(\frac{\omega}{c} r\right)}_{\text{Expansion coefficient Bessel function}} \underbrace{e^{im\phi}}_{\text{Circular harmonics}} & \mathbf{x} = (r, \phi, z) \\ &= e^{-i\langle \mathbf{k}_{pw}, \mathbf{x}_c \rangle} \sum_{m=-\infty}^{\infty} i^{-m} e^{im\phi_{pw}} J_m\left(\frac{\omega}{c} r'\right) e^{im\phi'} & \mathbf{x} - \mathbf{x}_c = (r', \phi', z') \text{ spatial shift} \\ &\approx e^{-i\langle \mathbf{k}_{pw}, \mathbf{x}_c \rangle} \sum_{m=-M}^{M} i^{-m} e^{im\phi_{pw}} J_m\left(\frac{\omega}{c} r'\right) e^{im\phi'} & \text{spatial band-limitation} \end{aligned}$$

Inverse Fourier Transform of the Bessel Functions

- circular harmonics expansion

$$S_{\text{pw}}^{(M)}(\mathbf{x}, \omega) = e^{-i\frac{\omega}{c} \langle \mathbf{n}_{\text{pw}}, \mathbf{x}_c \rangle} \sum_{m=-M}^M i^{-m} e^{-im\phi_{\text{pw}}} J_m\left(\frac{\omega}{c} r'\right) e^{im\phi'}$$

- forward Fourier transform of the Bessel function [Abramowitz and Stegun, 1964]

$$\mathcal{F}\{J_m(t)\} = \int_{-\infty}^{\infty} J_m(t) e^{-i\omega t} dt = \frac{2(-i)^m \Pi(\omega) T_m(\omega)}{\sqrt{1 - \omega^2}}$$

- exploiting the duality of Fourier transform, the inverse Fourier transform of $J_m\left(\frac{\omega}{c} r\right)$ reads

$$\mathcal{F}^{-1}\left\{J_m\left(\frac{\omega}{c} r\right)\right\} = \frac{i^m}{\pi} \frac{\Pi\left(\frac{ct}{2r}\right) T_m\left(\frac{ct}{r}\right)}{\sqrt{\left(\frac{r}{c}\right)^2 - t^2}}$$

$T_m(\cdot)$ Chebyshev polynomial of the first kind of degree m

$\Pi(\cdot)$ rectangular function

Time Domain Representations

$$S(x, \omega) = \sum_{m=-M}^M i^{-m} e^{-im\phi_{pw}} J_m(\frac{\omega}{c} r') e^{im\phi'}$$

↓ Plane Wave Decomposition

$$S(x, \omega) = \frac{1}{2\pi} \int_0^{2\pi} \mathcal{D}_M(\alpha - \phi_{pw}) e^{-i\frac{\omega}{c} \cos(\phi - \alpha)} d\alpha$$

↓ \mathcal{F}_t^{-1}

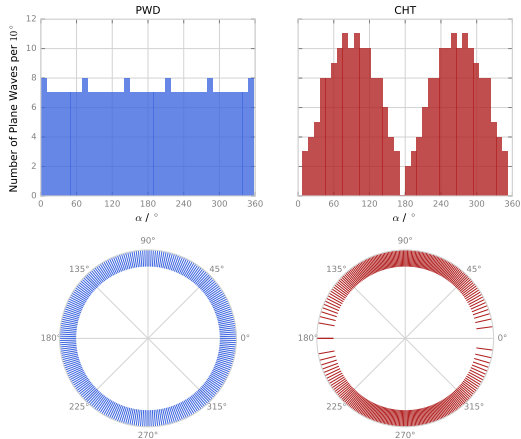
$$s(x, t) = \frac{1}{2\pi} \int_0^{2\pi} \mathcal{D}_M(\alpha - \phi_{pw}) \delta(t - \frac{r}{c} \cos(\phi - \alpha)) d\alpha$$

↓ sifting property of $\delta(\cdot)$

$$\begin{aligned} s(x, t) = & \frac{1}{2\pi} \frac{\pi(\frac{ct}{2r})}{|\sin \beta(t)|} [\mathcal{D}_M(\phi - \phi_{pw} - \pi + \beta(t)) \\ & + \mathcal{D}_M(\phi - \phi_{pw} - \pi - \beta(t))] \end{aligned}$$

\mathcal{F}_t^{-1}

Distribution of Plane Wave Directions

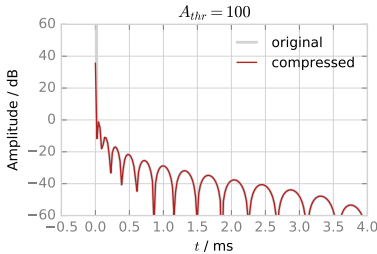
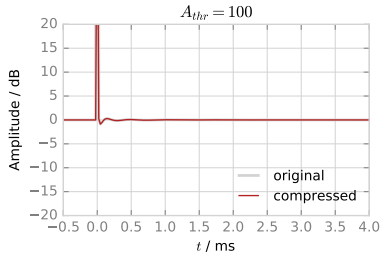


$$[x_c = (0.5, 0, 0), \phi_{pw} = -90^\circ, N_{pw} = 258]$$

- PWD: uniform distribution
- CHT: non-uniform distribution

Dynamic Range Control

only for CHT



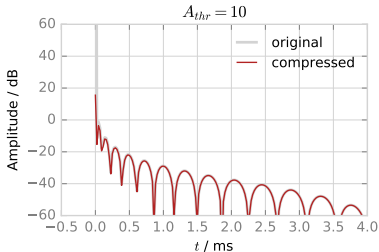
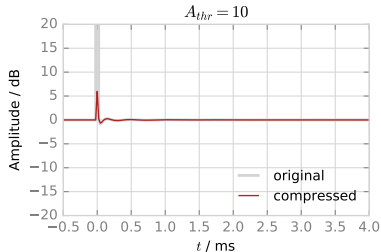
- $\frac{1}{|\sin \beta(t)|}$ tends to infinity for $t = \pm \frac{r}{c}$
- amplification of high frequency energy due to temporal aliasing
- soft-knee limiting function with empirically chosen A_{thr}

$$\mathcal{L}(u) = \frac{2A_{thr}}{\pi} \arctan \left(\frac{\pi u}{2A_{thr}} \right)$$

- low-pass filtering → reduce temporal aliasing artifacts

Dynamic Range Control

only for CHT



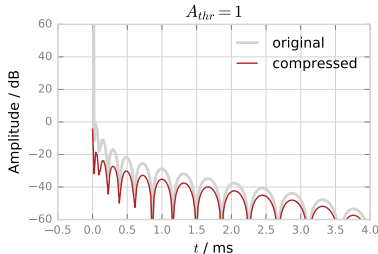
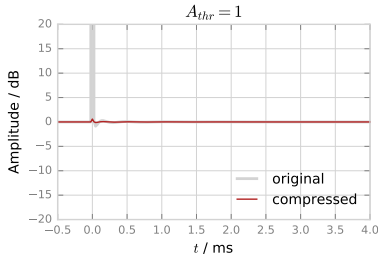
- $\frac{1}{|\sin \beta(t)|}$ tends to infinity for $t = \pm \frac{r}{c}$
- amplification of high frequency energy due to temporal aliasing
- soft-knee limiting function with empirically chosen A_{thr}

$$\mathcal{L}(u) = \frac{2A_{thr}}{\pi} \arctan \left(\frac{\pi u}{2A_{thr}} \right)$$

- low-pass filtering → reduce temporal aliasing artifacts

Dynamic Range Control

only for CHT



- $\frac{1}{|\sin \beta(t)|}$ tends to infinity for $t = \pm \frac{r}{c}$
- amplification of high frequency energy due to temporal aliasing
- soft-knee limiting function with empirically chosen A_{thr}

$$\mathcal{L}(u) = \frac{2A_{thr}}{\pi} \arctan \left(\frac{\pi u}{2A_{thr}} \right)$$

- low-pass filtering → reduce temporal aliasing artifacts

Frequency-Domain Driving Functions [Hahn et al., 2016]

$$D_{2D}(x_0, \omega) = -2a(x_0) \sum_{\mu=-N}^N \check{S}_\mu(\omega) e^{i\mu\varphi_0}$$

$$\times \left[\langle \hat{e}_r, n_0 \rangle \frac{\omega}{2c} \left\{ J_{\mu-1}(\frac{\omega}{c}\rho_0) - J_{\mu+1}(\frac{\omega}{c}\rho_0) \right\} + \langle \hat{e}_\varphi, n_0 \rangle i\mu J_\mu(\frac{\omega}{c}\rho_0) \right]$$

$$D_{3D}(x_0, \omega) = -2a(x_0) \sum_{n=0}^N \sum_{m=-n}^n \check{S}_n^m(\omega)$$

$$\left[\langle \hat{e}_r, n_0 \rangle \frac{1}{2n+1} \frac{\omega}{c} \left\{ nj_{n-1}(\frac{\omega}{c}r_0) - (n+1)j_{n+1}(\frac{\omega}{c}r_0) \right\} Y_n^m(\theta_0, \phi_0) \right.$$

$$+ \langle \hat{e}_\theta, n_0 \rangle \frac{-1}{r_0 \sin^2 \theta_0} j_n(\frac{\omega}{c}r_0) \left\{ (n+1) \cos \theta_0 Y_n^m(\theta_0, \phi_0) - \sqrt{\frac{2n+1}{2n+3} ((n+1)^2 - m^2)} Y_{n+1}^m(\theta_0, \phi_0) \right\}$$

$$\left. + \langle \hat{e}_\phi, n_0 \rangle \frac{im}{r_0 \sin \theta_0} j_n(\frac{\omega}{c}r_0) Y_n^m(\theta_0, \phi_0) \right]$$

$$D_{2.5D}(x_0, \omega) = \sqrt{\frac{2\pi\|x-x_0\|}{i\frac{\omega}{c}}} \times D_{2D}(x_0, \omega)$$

$$D_{2.5D}(x_0, \omega) = -2a(x_0) \sum_{m=-N}^N \frac{\check{S}_{|m|}^m(\omega) e^{im\varphi_0}}{4\pi i^{|m|-m} Y_{|m|}^{-m}(\frac{\pi}{2}, 0)}$$

$$\times \left[\langle \hat{e}_r, n_0 \rangle \frac{\omega}{2c} \left\{ J_{m-1}(\frac{\omega}{c}\rho_0) - J_{m+1}(\frac{\omega}{c}\rho_0) \right\} + \langle \hat{e}_\varphi, n_0 \rangle im J_m(\frac{\omega}{c}\rho_0) \right]$$